Performance and Optimization of Cooperative Diversity Systems in Generic Noise and Interference[1]

Amir Nasri, Robert Schober, and Ian F. Blake

Department of Electrical and Computer Engineering

The University of British Columbia

E-mail: {amirn, rschober, ifblake}@ece.ubc.ca

Abstract

Cooperative diversity systems have received significant attention recently as a distributed means of exploiting the inherent spatial diversity of wireless networks. In this paper, we consider a cooperative diversity system consisting of a source, a destination, and multiple single–hop amplify–and–forward relays, and provide a mathematical framework for the asymptotic analysis of this system in generic noise and interference for high signal–to–noise ratios. Assuming independent Rayleigh fading for all links in the network, we obtain simple and elegant closed–form expressions for the asymptotic symbol and bit error rates valid for arbitrary linear modulation formats, arbitrary numbers of relays, and arbitrary types of noise and interference with finite moments including co–channel interference, ultra–wideband interference, impulsive ϵ–mixture noise, generalized Gaussian noise, and Gaussian noise. Furthermore, we exploit the derived analytical error rate expressions to develop power allocation, relay selection, and relay placement schemes that are optimal in environments with generic noise and interference. Simulation results confirm our analysis and illustrate that, in non–Gaussian noise, the proposed power allocation, relay selection, and relay placement schemes lead to large performance gains compared to their conventional counterparts optimized for Gaussian noise.

[1] This paper has been accepted for presentation in part at the IEEE International Communications Conference (ICC), Cape Town, South Africa, May 2010.

1 Introduction

Cooperative diversity is a promising approach to achieve high diversity gains in distributed wireless networks where nodes are allowed to cooperate by relaying each other's messages. The main idea behind this technique is to allow idle wireless nodes to relay signals emitted by a source node to the destination node. As a result, the message transmitted by the source undergoes multiple independent fading paths and the probability of an erroneous decision at the destination is significantly reduced [1]. The two most popular relaying techniques are amplify–and–forward (AF) relaying and decode–and–forward (DF) relaying. While in DF relaying the signal received from the source is decoded and re–encoded at the relays, it is only amplified in AF relaying. Thus, AF relaying is generally considered to be less complex and is particularly well–suited for applications with simple relay units such as wireless sensor networks.

The performance of cooperative AF relay systems has been extensively studied in the literature. In particular, the outage probability for these systems has been calculated in [2, 3] and their capacity and outage capacity behavior have been analyzed in [4, 5] and [6], respectively. Furthermore, several exact and asymptotic results exist for the probability of error of cooperative diversity systems with AF relaying, see e.g. [7]–[11] and the references therein. These analytical results have subsequently been used to find optimal power allocation, relay selection, and relay placement strategies [8], [12]–[14]. While [1]–[14] and the vast body of related literature assume that the noise processes at the relays and the destination are Gaussian distributed, practical wireless systems are also impaired by *non–Gaussian* noise and interference. In fact, due to the distributed nature of wireless relay networks, the noise distributions at different network nodes may be different in general. Examples for non–Gaussian noise and interference that affect practical cooperative diversity systems include co–channel interference [15, 16], man–made impulsive noise [17, 18], and ultra–wideband (UWB) interference [19]. Thus, the analysis and optimization of cooperative diversity systems in the presence of *generic* noise[2] is of both theoretical and practical importance.

In this paper, we provide a unified mathematical framework for the analysis of the asymptotic performance of cooperative diversity systems impaired by generic noise. The main restriction imposed on the considered types of noise is that their statistical moments are finite, which is valid for noises of practical interest. The developed framework is general enough to take into account arbitrary numbers of relays and possibly different noise distributions at all network nodes. Based on the

[2]In the rest of this paper, the term "noise" refers to any additive impairment of the received signal, and also includes what is commonly referred to as "interference".

proposed framework, we derive closed–form expressions for the asymptotic symbol error rate (SER) and bit error rate (BER) of cooperative diversity systems impaired by Rayleigh fading and generic noise for high signal–to–noise ratios (SNR). The developed asymptotic performance results provide significant insight into the impact of system parameters such as the modulation format, the number of relays, and the type of noise on the overall system performance. In particular, these results reveal that the diversity gain achieved by cooperative diversity systems is equal to the number of paths between the source and the destination for all types of noise with finite moments. In contrast, the combining gain is significantly affected by the type of noise as it depends on certain noise moments.

Furthermore, we exploit the derived analytical results for optimization of cooperative diversity systems in generic noise. In particular, we develop optimal power allocation, relay selection, and relay placement strategies. Surprisingly, compared to their conventional counterparts developed for Gaussian noise, these novel schemes require only additional knowledge of certain noise moments, i.e., the additional signaling overhead is small. Our simulation results confirm the validity of the derived analytical SER and BER expressions and show that, in non–Gaussian noise, the proposed power allocation, relay selection, and relay placement strategies can yield significant performance gains over their conventional counterparts, which were developed for Gaussian noise.

The remainder of this paper is organized as follows. In Section 2, the system model for the considered cooperative diversity system is introduced. Asymptotic expressions for the SER and the BER performance are developed in Section 3. In Section 4, power allocation, relay selection, and relay placement strategies for non–Gaussian environments are developed. Numerical and simulation results are presented in Section 5, and some conclusions are drawn in Section 6.

Notation: In this paper, $(\cdot)^*$, $\Re\{\cdot\}$, $\mathcal{E}_x\{\cdot\}$, $\Gamma(\cdot)$, and ${}_2\mathcal{F}_1(\cdot,\cdot;\cdot;\cdot)$ denote complex conjugation, the real part of a complex number, statistical expectation with respect to x, the Gamma function, and the Gaussian hypergeometric function, respectively. We use the notation $u \overset{\circ}{=} v$ to indicate that u and v are asymptotically equivalent, and a function $f(x)$ is $o(g(x))$ if $\lim_{x\to 0} f(x)/g(x) = 0$.

2 System Model

The considered system consists of one source terminal, K relays, and one destination terminal. Transmission from the source to the destination is organized in two hops. In the first hop, the source transmits and the K relays and the destination receive, i.e., we assume that there is a direct link between the source and the destination. In the second hop, the relays amplify the signal received from the source and forward it to the destination. In order to prevent the relays from receiving the signal transmitted by other relays we assume that the source and the relays employ orthogonal channels, i.e., the relays transmit in e.g. different time slots or different frequency bands [2, 7, 8]. Thus, assuming perfect synchronization and demodulation at the relays and destination, the signal received at the destination in the first hop, r_0, and the signal received from relay k, $1 \leq k \leq K$, at the destination in the second hop, r_k, can be modeled as

$$\begin{aligned} r_0 &= \sqrt{P_0}\, h_0 x + n_0, && (1) \\ r_k &= A_k\, h_{2k} u_k + n_{2k}, \qquad 1 \leq k \leq K, && (2) \end{aligned}$$

where

$$u_k = \sqrt{P_0}\, h_{1k} x + n_{1k}, \qquad 1 \leq k \leq K, \tag{3}$$

is the received signal at the kth relay in the first hop. Here, P_0 is the average transmit symbol power of the source and A_k denotes the amplification gain of the kth relay. The symbol x transmitted by the source is taken from an M–ary alphabet $\mathcal{A}$ and is normalized such that $\mathcal{E}\{|x|^2\} = 1$. Furthermore, h_0, h_{1k}, and h_{2k} denote the fading gains of the source–destination channel, the channel between the source and relay k, and the channel between relay k and the destination, respectively. n_0, n_{1k}, and n_{2k} denote the (possibly) non–Gaussian distributed noise samples at the destination in the first hop, relay k in the first hop, and the destination in the second hop, respectively.

In the remainder of this section, we discuss the assumed fading and noise models, the amplification gain, and the diversity combining at the receiver in more detail.

Fading Model: We assume independent Rayleigh fading for all transmitter–receiver pairs [2, 7]. Thus, the fading gains $h_0 \triangleq a_0\, \mathrm{e}^{-j\theta_0}$, $h_{1k} \triangleq a_{1k}\, \mathrm{e}^{-j\theta_{1k}}$, and $h_{2k} \triangleq a_{2k}\, \mathrm{e}^{-j\theta_{2k}}$ are independent Gaussian random variables with zero mean and variances $\Omega_0 \triangleq \mathcal{E}\{|h_0|^2\}$, $\Omega_{1k} \triangleq \mathcal{E}\{|h_{1k}|^2\}$, and $\Omega_{2k} \triangleq \mathcal{E}\{|h_{2k}|^2\}$, respectively. The channel amplitudes a_0, a_{1k}, and a_{2k} are positive real random variables and follow a Rayleigh distribution. Furthermore, the channel phases θ_0, θ_{1k}, and θ_{2k} are uniformly distributed in $[-\pi, \pi)$ and are independent from the channel amplitudes.

Noise Model: The noise variances are denoted by $\sigma_{n_0}^2 \triangleq \mathcal{E}\{|n_0|^2\}$, $\sigma_{n_{1k}}^2 \triangleq \mathcal{E}\{|n_{1k}|^2\}$, and $\sigma_{n_{2k}}^2 \triangleq \mathcal{E}\{|n_{2k}|^2\}$, respectively. The distributed nature of the wireless relay network implies that the noise samples at different network nodes are statistically independent and have possibly different distributions. Furthermore, the noise samples relevant for different links and different hops at the destination, i.e., n_0 and n_{2k}, $1 \leq k \leq K$, may be identically or non–identically distributed. In particular, if the relays use a time–division multiple access approach for communication with the destination, the noise samples at the destination in different time slots will likely be identically distributed. In contrast, if the relays use frequency–division multiple access, different relay–destination links may be affected by different types of noise. For example, a co–channel interferer may affect one relay–destination frequency channel but not the others. For the analysis presented in Section 3 to be valid, we require all noise moments to exist. This is a mild condition which is met by most practically relevant types of noise and interference. Examples include (impulsive) ϵ–mixture noise, co–channel interference, generalized Gaussian noise, and UWB interference. Details about these and other types of non–Gaussian noise can be found in e.g. [20, 21].

Amplification Gain: For the amplification gain of the kth relay, A_k, several choices have been proposed in the literature. The most widely used choice is [2, 7, 8]

$$A_k = \sqrt{\frac{P_k}{P_0\, a_{1k}^2 + \sigma_{n_{1k}}^2}}, \tag{4}$$

which maintains a constant average transmit power P_k at the kth relay. As the above choice for the relay gain does not usually lead to a tractable mathematical analysis, it is customary in the literature to approximate this relay gain as [2, 7, 8]

$$A_k = \sqrt{\frac{P_k}{P_0 a_{1k}^2}}. \tag{5}$$

For the error rate performance analysis in Section 3, we also adopt (5) for the relay gain. Since (5) results in an increase in the relay transmit power compared to (4), the approximation involved in (5) leads to a lower bound on the error rate of the actual system that uses (4) for the relay gain. However, as will be shown in Section 5, this lower bound is very tight for sufficiently high SNRs.

Diversity Combining: We assume that the exact noise distributions at the relays and the destination are not known at the destination. Thus, the receiver at the destination employs maximum–ratio combining (MRC) to combine the $K+1$ received signal replicas, which is optimal for Gaussian noise. By rewriting (2) as

$$r_k = \sqrt{P_0} A_k\, h_{2k}\, h_{1k} x + \tilde{n}_k, \qquad 1 \le k \le K, \tag{6}$$

where $\tilde{n}_k \triangleq A_k\, h_{2k} n_{1k} + n_{2k}$, the MRC decision metric can be expressed as

$$m_c(\tilde{x}) = \frac{|r_0 - \sqrt{P_0} h_0 \tilde{x}|^2}{\sigma_{n_0}^2} + \sum_{k=1}^{K} \frac{|r_k - \sqrt{P_0} A_k\, h_{2k}\, h_{1k} \tilde{x}|^2}{\sigma_{\tilde{n}_k}^2} \tag{7}$$

where $\tilde{x} \in \mathcal{A}$ is a trial symbol and we have defined

$$\sigma_{\tilde{n}_k}^2 \triangleq \sigma_{n_{2k}}^2 + A_k^2\, a_{2k}^2\, \sigma_{n_{1k}}^2, \qquad 1 \le k \le K. \tag{8}$$

The MRC detector decides in favor of that trial symbol $\tilde{x}$ which minimizes $m_c(\tilde{x})$.

3 Error Rate Analysis

For the analysis presented in this section, it is convenient to define the instantaneous SNRs of the source–destination link, the source–relay links, and the relay–destination links as $\gamma_0 \triangleq P_0\, a_0^2/\sigma_{n_0}^2$, $\gamma_{1k} \triangleq P_0\, a_{1k}^2/\sigma_{n_{1k}}^2$, and $\gamma_{2k} \triangleq P_k\, a_{2k}^2/\sigma_{n_{2k}}^2$, respectively. The corresponding average SNRs are given by $\bar{\gamma}_0 = P_0\,\Omega_0/\sigma_{n_0}^2$, $\bar{\gamma}_{1k} = P_0\,\Omega_{1k}/\sigma_{n_{1k}}^2$, and $\bar{\gamma}_{2k} = P_k\,\Omega_{2k}/\sigma_{n_{2k}}^2$. In addition, we introduce the normalized noise samples $\bar{n}_0 \triangleq n_0/\sigma_{n_0}$ and $\bar{n}_{ik} \triangleq n_{ik}/\sigma_{n_{ik}}$, $i = 1, 2$, $1 \le k \le K$.

In the following, we analyze the asymptotic error rate performance of the considered cooperative diversity system for $\bar{\gamma}_0, \bar{\gamma}_{1k}, \bar{\gamma}_{2k} \to \infty$, $1 \le k \le K$. In particular, we develop asymptotic expressions for the pairwise error probability (PEP) and relate these PEPs to the respective asymptotic SERs and BERs.

3.1 Asymptotic PEP

Assuming that $x \in \mathcal{A}$ was transmitted and $\hat{x} \in \mathcal{A}$, $\hat{x} \neq x$ was detected, the PEP for the considered cooperative diversity system can be expressed as

$$P_e(d) = \Pr\{m_c(x) > m_c(\hat{x})\}, \tag{9}$$

where $d = |e|$ and $e = x - \hat{x}$. It is convenient to first obtain the PEP conditioned on noise vector $\boldsymbol{n} = [n_0\ n_{11}\ n_{21}\ \ldots\ n_{1K}\ n_{2K}]$, which collects all noise components of the considered system. This conditional PEP can be expressed as

$$P_e(d|\boldsymbol{n}) = \Pr\{m_c(x) > m_c(\hat{x})|\boldsymbol{n}\} = \Pr\left\{\sum_{k=0}^{K} \Delta_k < 0\right\} \tag{10}$$

where

$$\Delta_k \triangleq \begin{cases} \left(|\sqrt{P_0} h_0\, e + n_0|^2 - |n_0|^2\right)/\sigma_{n_0}^2, & k = 0, \\ \left(|\sqrt{P_0} A_k\, h_{2k}\, h_{1k} e + \tilde{n}_k|^2 - |\tilde{n}_k|^2\right)/\sigma_{\tilde{n}_k}^2, & 1 \le k \le K. \end{cases} \tag{11}$$

Based on (10) the conditional PEP can be expressed as [22]

$$P_e(d|\boldsymbol{n}) = \frac{1}{2\pi j} \int_{c-j\infty}^{c+j\infty} \Phi(s|\boldsymbol{n})\, \frac{\mathrm{d}s}{s}, \tag{12}$$

where c is a small positive constant that lies in the region of convergence of the integrand. In the above equation we have introduced the moment generating function (MGF) $\Phi(s|\boldsymbol{n}) \triangleq \prod_{k=0}^{K} \Phi_{\Delta_k}(s|\boldsymbol{n})$ with $\Phi_{\Delta_k}(s|\boldsymbol{n}) \triangleq \mathcal{E}_{\boldsymbol{a},\boldsymbol{\theta}}\{e^{-s\Delta_k}\}$, where $\boldsymbol{a} \triangleq [a_0\ a_{11}\ a_{21}\ \ldots\ a_{1K}\ a_{2K}]$ and $\boldsymbol{\theta} \triangleq [\theta_0\ \theta_{11}\ \theta_{21}\ \ldots\ \theta_{1K}\ \theta_{2K}]$ denote the channel amplitude vector and the channel phase vector, respectively. By the *residue theorem* [22], the conditional PEP in (12) is given by the sum of the residues of $\Phi(s|\boldsymbol{n})/s$ at poles lying in the left hand side of the complex s–plain (including the imaginary axis). In order to investigate the singularities of $\Phi(s|\boldsymbol{n})/s$, we provide the asymptotic Laurent series representations of $\Phi_{\Delta_0}(s|\boldsymbol{n})$ and $\Phi_{\Delta_k}(s|\boldsymbol{n})$, $1 \leq k \leq K$, around $s = 0$ in the following two lemmas:

Lemma 1: The asymptotic Laurent series expansion of $\Phi_{\Delta_0}(s|\boldsymbol{n})$ around $s = 0$ for $\bar{\gamma}_0 \to \infty$ is given by

$$\Phi_{\Delta_0}(s|\boldsymbol{n}) = \frac{1}{d^2 s \bar{\gamma}_0} \sum_{\xi=0}^{\infty} \frac{1}{\xi!} s^{\xi} |\bar{n}_0|^{2\xi} + o(\bar{\gamma}_0^{-1}). \tag{13}$$

Proof: The asymptotic Laurent series expansion in (13) can be calculated following the same steps as in [23, Section IV.A]. In particular, (13) can be obtained from [23, Eq. (14)] by adjusting the notation of [23] to the problem at hand. □

Lemma 2: For $1 \leq k \leq K$, the asymptotic Laurent series expansion of $\Phi_{\Delta_k}(s|\boldsymbol{n})$ around $s = 0$ for $\bar{\gamma}_{1k}, \bar{\gamma}_{2k} \to \infty$ is given by

$$\Phi_{\Delta_k}(s|\boldsymbol{n}) = \frac{1}{d^2 s} \sum_{\xi=0}^{\infty} \frac{1}{\xi!} s^{\xi} \left(\frac{|\bar{n}_{1k}|^{2\xi}}{\bar{\gamma}_{1k}} + \frac{|\bar{n}_{2k}|^{2\xi}}{\bar{\gamma}_{2k}} \right) + o(\bar{\gamma}_{1k}^{-1}) + o(\bar{\gamma}_{2k}^{-1}). \tag{14}$$

Proof: Please refer to the Appendix. □

Using d'Alembert's convergence test [24, 0.222] it can be shown that the series in (13) and (14) are convergent for all $s \neq 0$. It follows that all singularities of $\Phi(s|\boldsymbol{n})/s = \prod_{k=0}^{K} \Phi_{\Delta_k}(s|\boldsymbol{n})/s$ are located at $s = 0$. Thus, the conditional PEP is given by the residue of $\Phi(s|\boldsymbol{n})/s$ at $s = 0$ or equivalently by the coefficient associated with s^0 in the series expansion of $\Phi(s|\boldsymbol{n})$. The series expansion of $\Phi(s|\boldsymbol{n})$ can be found by combining (13) and (14) leading to the following result for the asymptotic conditional PEP:

$$P_e(d|\boldsymbol{n}) = \frac{1}{d^{2(K+1)}} \sum_{i_0+\cdots+i_K=K+1} \frac{|\bar{n}_0|^{2i_0}}{\bar{\gamma}_0 i_0!} \prod_{k=1}^{K} \frac{1}{i_k!} \left(\frac{|\bar{n}_{1k}|^{2i_k}}{\bar{\gamma}_{1k}} + \frac{|\bar{n}_{2k}|^{2i_k}}{\bar{\gamma}_{2k}} \right) + o\left(\frac{1}{\bar{\gamma}_0} \prod_{k=1}^{K} \frac{1}{\min\{\bar{\gamma}_{1k}, \bar{\gamma}_{2k}\}} \right). \tag{15}$$

Averaging the expression in (15) with respect to the noise leads to the unconditional asymptotic PEP

$$P_e(d) = \mathcal{E}_{\boldsymbol{n}}\{P_e(d|\boldsymbol{n})\} \doteq \frac{1}{d^{2(K+1)}} \sum_{i_0+\cdots+i_K=K+1} \frac{m_0(i_0)}{\bar{\gamma}_0 i_0!} \prod_{k=1}^{K} \frac{1}{i_k!}\left(\frac{m_{1k}(i_k)}{\bar{\gamma}_{1k}} + \frac{m_{2k}(i_k)}{\bar{\gamma}_{2k}}\right), \tag{16}$$

where we have introduced the (normalized) noise moments $m_0(i) \triangleq \mathcal{E}\{|\bar{n}_0|^{2i}\}$, $m_{1k}(i) \triangleq \mathcal{E}\{|\bar{n}_{1k}|^{2i}\}$, and $m_{2k}(i) \triangleq \mathcal{E}\{|\bar{n}_{2k}|^{2i}\}$, and used the fact that the normalized noise samples $\bar{n}_0$, $\bar{n}_{1k}$, and $\bar{n}_{2k}$ are statistically independent.[3] Since we have absorbed terms containing $|\bar{n}_0|^\nu$, $|\bar{n}_{1k}|^\nu$, and $|\bar{n}_{2k}|^\nu$, $\nu > 0$, in the $o(\cdot)$ terms in (15), we require all noise moments to be finite for (16) to be valid. We note that this mild condition holds for all noises of practical interest and analytical expressions for their moments can be usually easily obtained, see [21, Table II] for examples. If the noise moments can not be obtained analytically, they can be conveniently calculated by Monte–Carlo simulation.

3.2 Asymptotic SER and BER

The asymptotic SER, P_s, can be obtained from the asymptotic PEP as [25]

$$P_s \doteq \zeta_m P_e(d_m), \tag{17}$$

where d_m and ζ_m are modulation dependent parameters that denote the minimum Euclidean distance and the average number of minimum–distance neighbors of signal constellation $\mathcal{A}$, respectively. These parameters are listed in [21, Table I] for commonly used signal constellations such as M–ary quadrature amplitude modulation (M–QAM) and M–ary phase–shift keying (M–PSK). If the noise samples n_0, n_{1k}, and n_{2k}, are Gaussian distributed $m_0(i) = m_{1k}(i) = m_{2k}(i) = i!$ is valid and therefore the asymptotic SER can be obtained from (16) and (17) as

$$P_s \doteq \frac{\zeta_m}{d_m^{2(K+1)}} \binom{2K+1}{K} \frac{1}{\bar{\gamma}_0} \prod_{k=1}^{K} \left(\frac{1}{\bar{\gamma}_{1k}} + \frac{1}{\bar{\gamma}_{2k}}\right). \tag{18}$$

Eq. (18) is equivalent to (but in somewhat simpler form than) [8, Eq. (33)][4]. We emphasize, however, that the analysis in [8] is not applicable to the scenario considered in this paper as it is limited to additive white Gaussian noise (AWGN). Finally, the asymptotic BER, P_b, can be approximated as [25]

$$P_b \doteq \frac{\zeta_m}{\log_2(M_{\mathcal{A}})} P_e(d_m), \tag{19}$$

[3] We note that the assumption of statistical independent noise is not necessary but simplifies the final expression for the asymptotic PEP. In particular, if the noise samples in (15) were statistically dependent, their joint moments would appear in the asymptotic PEP expression.

[4] Note that k used in [8, Eq. (33)] is equal to $k = 2d_m^2$.

where $M_{\mathcal{A}}$ is the size of constellation $\mathcal{A}$. If Gray labeling is used, (19) becomes accurate for high SNRs. Intuitively, we can say that the heavier the tails of a certain type of noise are, the larger are its higher order moments for a given variance. Therefore, from (16), (17), and (19) we expect that the heavier the tails of a certain type of noise are, the poorer its BER and SER performance will be.

3.3 Diversity Gain and Combining Gain

To get more insight into the system performance, we express the asymptotic BER in terms of the diversity gain G_d and the combining gain G_c. In particular, following [7], we let $\bar{\gamma}_{1k} = \bar{\gamma}_{2k} = \bar{\gamma}_0 = \bar{\gamma}$, and express the asymptotic BER as $P_b \doteq (G_c \bar{\gamma})^{-G_d}$. G_d and G_c correspond to the negative asymptotic slope and a relative horizontal shift of the BER curve when plotted as a function of the SNR $\bar{\gamma}$ on a double–logarithmic scale, respectively. Based on (16) and (19), it is easy to see that the diversity gain is given by $G_d = K + 1$ regardless of the type of noise. We note that this result was previously known to hold for impairment by Gaussian noise [7, 8] but our analysis shows that it holds for a much larger class of noises (all noises with finite moments). In contrast, we observe from (16) and (19) that the combining gain G_c does depend on the type of noise via the noise moments. Thus, on a double–logarithmic scale we expect the BER curves for different types of noise to be parallel and their relative horizontal shift to depend on the moments of the noise.

4 Optimization of Cooperative Diversity Systems

In this section, we exploit the analytical performance results obtained in the previous section for the design and optimization of cooperative diversity systems impaired by generic noise. In particular, we consider the problems of optimizing power allocation, relay section, and relay placement.

4.1 Power Allocation

Power allocation for cooperative diversity systems impaired by Gaussian noise has been extensively studied in the literature for various performance criteria such as capacity, outage probability, and SER, see e.g. [12]–[14] and references therein. Here, we are interested in optimizing the powers P_k, $0 \leq k \leq K$, allocated to the source and the relay nodes for minimization of the asymptotic SER derived in Section 3. In particular, using (16) and (17) the corresponding optimization problem can be formulated as

$$\min_{P_0,\dots,P_K} \sum_{i_0+\cdots+i_K=K+1} \frac{m_0(i_0)}{i_0! P_0} \prod_{k=1}^{K} \frac{1}{i_k!} \left(\frac{m_{1k}(i_k)}{P_0 \xi_{1k}} + \frac{m_{2k}(i_k)}{P_k \xi_{2k}} \right) \tag{20}$$

$$\text{s.t.} \quad \sum_{k=0}^{K} P_k \leq P_T \tag{21}$$

$$P_{\min,k} \leq P_k \leq P_{\max,k} \quad 0 \leq k \leq K, \tag{22}$$

where $\xi_{1k} \triangleq \Omega_{1k}/\sigma^2_{n_{1k}}$ and $\xi_{2k} \triangleq \Omega_{2k}/\sigma^2_{n_{2k}}$ depend on the channel statistics, $P_{\min,k}$ and $P_{\max,k}$ denote, respectively, the minimum and the maximum powers that can be allocated to node k, and P_T denotes the total power budget. We note that (20)–(22) comprise a large class of power allocation problems. For example, if individual relay power constraints are not required, we can simply set $P_{\min,k} = 0$ and $P_{\max,k} = \infty$, $\forall k$, and effectively omit constraint (22). On the other hand, if the power at the source or one of the relays is fixed to $\bar{P}_k$, we can set $P_{\min,k} = \bar{P}_k = P_{\max,k} - \epsilon$, where ϵ is a small number (e.g. 10^{-6}). Since both the objective function and the constraints in (20)–(22) are posynomials, the optimization problem in (20)–(22) is a geometric program [26], which can be efficiently solved numerically [27]. In the following, we refer to the solution of (20)–(22) as optimal power allocation (OPA). If the noise at all network nodes is assumed to be Gaussian, $m_0(i) = m_{1k}(i) = m_{2k}(i) = i!$, $1 \leq i \leq K$, holds and the corresponding solution of (20)–(22) is referred to as Gaussian power allocation (GPA) in the following. The power allocation is typically computed at the destination node, which forwards the solution to the relays and the source node. For computation of the GPA, the destination node requires only knowledge about the channel statistics ξ_{1k} and ξ_{2k}, $1 \leq k \leq K$ [12]. In contrast, for computation of the OPA, the destination node also has to know the noise moments $m_0(i)$, $m_{1k}(i)$, and $m_{2k}(i)$, $2 \leq i \leq K+1$, $1 \leq k \leq K$. The moments $m_0(i)$ and $m_{2k}(i)$, $1 \leq k \leq K$, can be estimated directly by the destination node, whereas the moments $m_{1k}(i)$ have to be estimated by relay k and subsequently fed back to the destination via a low–rate feedback link. Since the noise moments can be expected to change slowly with time, the additional signaling overhead required for OPA compared to GPA can be considered to be moderate.

Special Case ($K = 1$ Relay): To obtain more insight into the power allocation problem, we consider the special case of $K = 1$ relay and the absence of individual power constraints, i.e., $P_{\min,1} = 0$ and $P_{\max,1} = \infty$. In this case, the OPA problem reduces to

$$\min_{P_0,P_1} \quad \frac{1}{P_0} \left(\frac{1}{P_0} + \frac{\lambda \nu}{P_1} \right) \tag{23}$$

$$\text{s.t.} \quad P_0 + P_1 \leq P_T \tag{24}$$

with $\lambda \triangleq \frac{\Omega_{11}/\sigma_{n_{11}}^2}{\Omega_{21}/\sigma_{n_{21}}^2}$ and $\nu \triangleq (2+m_0(2)+m_{21}(2))/(2+m_0(2)+m_{11}(2))$. Here, $0<\lambda<\infty$ is a measure for the quality of the source–relay link compared to relay–destination link. For example, if both channels have the same quality, $\lambda=1$ holds. Furthermore, $0<\nu<\infty$ is a measure of the relative heaviness of the tails of the noise samples n_{11} and n_{21}. Denoting the optimal source and relay powers by P_0^* and P_1^*, respectively, and defining $\alpha^* \triangleq P_0^*/P_1^*$, the OPA can be obtained from (23) and (24) as $P_0^*=P_T/(1+\alpha^*)$ and $P_1^*=\alpha^* P_T/(1+\alpha^*)$, with

$$\alpha^* = \frac{1}{4}(-\lambda\nu + \sqrt{\lambda^2\nu^2+8\lambda\nu}). \tag{25}$$

Since $0 \le \alpha^* \le 1$ follows from (25), $P_0^* \ge P_1^*$ holds, i.e., the source is never allocated less power than the relay. Furthermore, α^* is an increasing function in both λ and ν. As a result, if λ increases, i.e., if the quality of the source–relay channel improves compared to the relay–destination channel, more power is allocated to the relay. In contrast, if ν decreases ($m_{11}(2)$ increases compared to $m_{21}(2)$), the power allocated to the relay is reduced. This implies that the OPA allocates less power to a relay impaired by noise with heavier tails (larger $m_{11}(2)$) compared to a relay impaired by noise with shorter tails (smaller $m_{11}(2)$).

For comparison, we also introduce the GPA for the case of one relay, which is given by $P_0 = P_T/(1+\alpha_{\mathrm{G}})$ and $P_1 = \alpha_{\mathrm{G}} P_T/(1+\alpha_{\mathrm{G}})$ [13], where

$$\alpha_{\mathrm{G}} = \frac{1}{4}(-\lambda + \sqrt{\lambda^2+8\lambda}). \tag{26}$$

We note that while the GPA does not depend on the properties of the source–destination link at all, the OPA is affected by the moment $m_0(2)$ of noise n_0 which impairs the source–destination link.

In practice, a cooperative diversity system which does not have access to the noise moments may apply GPA even if the noise has a non–Gaussian distribution or simply use equal power allocation (EPA) with $P_0=P_1=P_T/2$. Therefore, it is interesting to compare the performance of OPA with the performances of GPA and EPA. In particular, based on (16) and (17), we can show that the asymptotic performance gain of OPA over GPA, G_{OG}, and the performance gain of OPA over EPA, G_{OE}, is

$$G_{\mathrm{OG}}[\mathrm{dB}] = 5\log\left(\frac{\alpha^*(1+\alpha_{\mathrm{G}})^2\,(\alpha_{\mathrm{G}}+\lambda\nu)}{\alpha_{\mathrm{G}}(1+\alpha^*)^2\,(\alpha^*+\lambda\nu)}\right) \tag{27}$$

and

$$G_{\mathrm{OE}}[\mathrm{dB}] = 5\log\left(\frac{4\,\alpha^*\,(1+\lambda\nu)}{(1+\alpha^*)^2\,(\alpha^*+\lambda\nu)}\right), \tag{28}$$

respectively, i.e., for example, OPA requires a G_{OG} lower SNR to achieve the same SER as GPA. It can be shown that G_{OE} is a decreasing function of ν and furthermore $\lim_{\nu\to 0} G_{\mathrm{OE}} = 3\mathrm{dB}$ is valid, i.e., the maximum performance gain of OPA over EPA is 3 dB and is achieved if the tails of the noise at the relay are much heavier than the tails of the noise at the destination ($m_{11}(2)$ much larger than $m_0(2)$ and $m_{21}(2)$). On the other hand, G_{OG} is an increasing function of ν for $\nu \geq 1$ and a decreasing function of ν for $\nu \leq 1$, i.e., for a given λ, G_{OG} has local maxima at $\nu = 0$ and $\nu \to \infty$. One of these local maxima is also the global maximum. The behavior of G_{OG} and G_{OE} will be studied more in detail in Section 5.

4.2 Relay Selection

The performance of cooperative diversity systems has been shown to be limited by the orthogonal allocation of system resources [12]. This problem can be overcome by relay selection where only one out of the K available relays is selected for forwarding the message to the destination [12, 8]. Here, we propose a new relay selection scheme for cooperative diversity systems that are affected by generic noise. We assume that the destination, which performs the relay selection, knows the average SNRs of all links in the network (but not the instantaneous channel gains). For the Gaussian case, it was shown in [8] that the asymptotic SER is minimized by selecting relay $k_G = \underset{1 \leq k \leq K}{\operatorname{argmin}} \{\rho_{\mathrm{G}}(k)\}$, where

$$\rho_{\mathrm{G}}(k) = \bar{\gamma}_{1k}^{-1} + \bar{\gamma}_{2k}^{-1}. \tag{29}$$

In contrast, for non–Gaussian noise the relay that minimizes the asymptotic SER according to (16) and (17) is given by $k^* = \underset{1 \leq k \leq K}{\operatorname{argmin}} \{\rho_{\mathrm{NG}}(k)\}$, where

$$\rho_{\mathrm{NG}}(k) = [2 + m_0(2) + m_{1k}(2)]\, \bar{\gamma}_{1k}^{-1} + [2 + m_0(2) + m_{2k}(2)]\, \bar{\gamma}_{2k}^{-1}. \tag{30}$$

Eq. (30) is obtained by formally setting $K = 1$ in (16) since only one relay is selected. Compared to the Gaussian case in (29), for the proposed selection criterion in (30), the destination also has to know the noise moments $m_0(2)$, $m_{1k}(2)$, and $m_{2k}(2)$, $1 \leq k \leq K$, which can be obtained in the same manner as discussed for the power allocation problem in Section 4.1.

We note that, in general, the selection criteria in (29) and (30) are not equivalent and lead to different relays being selected. The two selection criteria are equivalent only for the special case when the noise moments at all nodes are identical, i.e., $m_{1k}(2) = m_{2k}(2) = m$, $1 \leq k \leq K$, where m is a constant and independent of k.

4.3 Relay Placement

Assuming that the relay(s) in the cooperative diversity system can be placed at an arbitrary location, it is interesting to find the placement which results in the lowest overall SER for the system [8]. To simplify our exposition, we confine our attention to a cooperative diversity system with a single relay where the relay is placed on the line connecting the source and the destination. We denote the source–relay and source–destination distances by d_{SR} and d_{SD}, respectively, their ratio by $\delta \triangleq d_{\mathrm{SR}}/d_{\mathrm{SD}}$, and the path–loss exponent by α_p . This implies $\Omega_{11} = \Omega_0/\delta^{\alpha_p}$ and $\Omega_{21} = \Omega_0/(1-\delta)^{\alpha_p}$. To find the relay placement that minimizes the SER for the considered cooperative diversity system, using (16) and (17), we obtain the optimization problem

$$\begin{aligned} \min_{\delta} \qquad & P_0^{-2}\sigma_{n_{11}}^2 [2+m_0(2)+m_{11}(2)]\,\delta^{\alpha_p} \\ & + P_0^{-1}P_1^{-1}\sigma_{n_{21}}^2 [2+m_0(2)+m_{21}(2)]\,(1-\delta)^{\alpha_p} \end{aligned} \tag{31}$$

If the relevant moments of the noise samples n_0, n_{11}, and n_{21} are independent of δ, the optimal value δ^* can be obtained as

$$\delta^* = \frac{1}{\left(\frac{\sigma_{n_{11}}^2 P_1}{\sigma_{n_{21}}^2 P_0\,\nu}\right)^{1/(\alpha_p-1)} + 1}, \tag{32}$$

where (as before) $\nu = (2+m_0(2)+m_{21}(2))/(2+m_0(2)+m_{11}(2))$ is a measure of the relative heaviness of the tails of the noise at the destination compared to the noise at the relay. δ^* is an increasing function of ν. If the noise at the destination in the second hop has very heavy tails compared to the noise at the destination in the first hop and the noise at the relay, i.e., $m_{21}(2) \gg m_0(2),\, m_{11}(2)$, the relay will be placed very close to the destination ($\delta^* \to 1$) to compensate for the severe impairment caused by the heavy–tailed noise in the second hop. On the other hand, if the noise at the relay has very heavy tails compared to the noise at the destination, i.e., $m_{11}(2) \gg m_0(2),\, m_{21}(2)$, the relay will be placed very close to the source ($\delta^* \to 0$) to compensate for the heavy tails of the noise at the relay. The optimal relay placement for Gaussian noise is obtained from (32) by letting $\nu = 1$ [8].

We note that in practice the noise statistics $\sigma_{n_{11}}^2$, $\sigma_{n_{21}}^2$, $m_0(2)$, $m_{11}(2)$, and $m_{21}(2)$ may not be independent of δ. For example, the effect of a co–channel interferer will depend on the location of the relay relative to the interferer. In this case, (32) is not valid but the optimal value δ^* can still be determined based on (31) using a one–dimensional search taking into account the dependence of the noise statistics on δ. A corresponding example will be discussed in Section 5.

5 Numerical and Simulation Results

In this section, we verify the analytical results derived in Section 3 with computer simulations and investigate the performance improvements achievable with the power allocation, relay selection, and relay placement strategies introduced in Section 4. Unless stated otherwise, we adopted equal powers for the source and all relays (i.e., $P_k = P_0$), unit variance for all channels (i.e., $\Omega_0 = \Omega_{1k} = \Omega_{2k} = 1$), and equal variances for all noise samples (i.e., $\sigma^2_{n_0} = \sigma^2_{n_{1k}} = \sigma^2_{n_{2k}} = N_0$, $1 \leq k \leq K$). The noise models and their parameters used in this section are described in detail in [20]. For all figures, the analytical results were obtained using (16), (17), and (19), and the parameters of the considered types of noise are specified in the captions of the figures.

In Fig. 1, we show the BER of a cooperative diversity system with $K = 2$ relays and BPSK modulation versus the average transmit SNR defined as $\gamma_t \triangleq P_0/N_0$. The noise samples n_0, n_{1k}, and n_{2k}, $1 \leq k \leq K$, are assumed to be identically distributed and results are shown for AWGN, unfaded and Rayleigh–faded co–channel interference (CCI), generalized Gaussian noise (GGN), ϵ–mixture noise, and impulse–radio (IR) UWB interference [20]. As seen from the figure, for high enough SNRs the simulation results are in good agreement with the analytical results. The small differences observed between simulation and analytical results at high SNRs are due to the fact that we have used the approximate relay amplification gain in (5) in our analysis instead of the actual gain in (4) which was used for all simulation results shown in this section. As expected from the analysis in Section 3.3, at high SNRs the BER curves are parallel and the cooperative diversity system achieves a diversity gain of $G_d = K + 1 = 3$ irrespective of the type of noise. Nevertheless, large differences in performance are observed for different types of noise due to the effect of the noise moments on the combining gain G_c.

The BERs of cooperative diversity systems employing 16–QAM modulation and different numbers of relays are shown in Fig. 2. Results are shown for the case where all network nodes are affected by ϵ–mixture noise and AWGN, respectively. Similar to Fig. 1, for high enough SNR the simulation results and the analytical results are in good agreement. Since the ϵ–mixture noise is impulsive, it causes a significant performance degradation compared to AWGN. However, for both types of noise increasing the number of relays yields a significant performance improvement, since the diversity gain $G_d = K + 1$ increases.

In Figs. 3 and 4, we consider the power allocation problem described in Section 4.1. In particular, in Fig. 3, we show the performance gains achievable with the proposed OPA scheme compared to GPA (G_{OG}) and EPA (G_{OE}) as obtained from (27) and (28), respectively, as functions of parameter

ν (a measure for the relative heaviness of the tails of the involved noises) for three values of relative channel–quality parameter λ. The gain of OPA compared to EPA is maximum if the noise at the relay has much heavier tails than the noise at the destination ($\nu \to 0$), and approaches zero if the noise in the second hop at the destination has much heavier tails than the noise at the relay and the noise at the destination in the first hop ($\nu \to \infty$) since EPA is the optimal strategy in this case. On the other hand, the gain of OPA compared to GPA has local maxima for $\nu \to 0$ and $\nu \to \infty$ and becomes zero if all nodes are impaired by the same type of noise ($\nu = 0$). For $\lambda = 10^3$, the quality of the source–relay channel is much better than the quality of the relay–destination channel. In this case, the GPA solution is identical to EPA and $G_{\mathrm{OG}} = G_{\mathrm{OE}}$.

In Fig. 4, we show the BER of a cooperative diversity system with $K = 2$ relays and BPSK modulation for OPA, GPA, and EPA ($P_0 = P_1 = P_2 = P_T/3$) versus P_T/N_0. We assume that the destination and all relays are impaired by AWGN, except the signal received from the first relay in the second hop at the destination is impaired by IR–UWB interference (n_{21}). Furthermore, we assume $\Omega_{21}/\Omega_{11} = 100$ and $\Omega_{22}/\Omega_{12} = 10$. For OPA and GPA we assumed that the individual power constraints in (22) were not in effect, and solved the remaining optimization problem (20), (21) using the geometric program solver in [27]. Fig. 4 shows that the asymptotic performance gains of OPA over GPA and EPA are 1.2 dB and 1.7 dB, respectively. To gain more insight, we consider the case of a total power budget of $P_T = 1$. In this case, the resulting optimal powers are ($P_0^* = 0.66, P_1^* = 0.22, P_2^* = 0.12$), while we obtain ($P_0 = 0.82, P_1 = 0.05, P_2 = 0.13$) for GPA and ($P_0 = P_1 = P_2 = 0.33$) for EPA. Since $\Omega_{21}/\Omega_{11} \gg \Omega_{22}/\Omega_{12}$ is valid, a very low power is allocated to the first relay by the GPA scheme, which assumes that all noise samples are Gaussian distributed. In contrast, the OPA scheme allocates more power to the first relay (and less power to the source) in order to compensate for the adverse effect of the impulsive IR–UWB interference, n_{21}, affecting the relay–destination link. We note that the relatively slow convergence of the simulation results to the asymptotic results in Fig. 4 is due to the fact that the source–destination channel is of very low quality (small Ω_{11}), and thus, large P_T are required to justify the high SNR assumption for this link.

In Fig. 5, we consider the relay selection problem discussed in Section 4.2. In particular, assuming that three relays are available for cooperation, we show the SER of 8–PSK modulation when each of these relays is selected. We assume that the noise samples at the destination n_0 and n_{2k}, $k = 1, 2, 3$, are Gaussian distributed. Relays 1, 2, and 3 are impaired by IR–UWB interference, ϵ–mixture noise, and unfaded CCI, respectively. For this scenario and $\gamma_t = 30$ dB, the values of the new selection criterion in (30) for the three relays are $\rho_{\mathrm{NG}}(1) = 2.74 \times 10^{-2}$, $\rho_{\mathrm{NG}}(2) = 1.23 \times 10^{-2}$, and $\rho_{\mathrm{NG}}(3) =$

0.55×10^{-2}, and therefore, relay 3 is selected. In contrast, for the conventional selection criterion in (29), which assumes a Gaussian distribution and ignores the true distribution of the noise, we have $\rho_{\mathrm{G}}(1) = \rho_{\mathrm{G}}(2) = \rho_{\mathrm{G}}(3) = 0.6 \times 10^{-2}$, i.e., this criterion equally favors the three relays implying that one of the relays has to be selected at random. Fig. 5 shows that if (29) is used instead of (30), a performance loss of more than 3 dB can be incurred at $\mathrm{SER} = 10^{-5}$ if relay 1 is selected instead of relay 3.

In Fig. 7, we study the performance of various relay placement strategies for the cooperative diversity system depicted in Fig. 6. The relay R and the destination D are affected by AWGN having variance N_0 and an impulsive interferer I emitting a power P_I. We model the interferer as ϵ–mixture noise ($\epsilon = 0.01$, $\kappa = 100$) which is a good model for certain types of UWB interference [28] and man–made interference [17]. For concreteness, we adopt a path–loss exponent of $\alpha_d = 4$ and the system parameters in [29], which leads to $N_0 = -95$ dBm. Furthermore, we assume $P_I = -58$ dBm and BPSK modulation. We note that, in this case, the total noise variance and the noise distribution at the relay are not independent of the location parameter δ, since the interference power at the relay depends on distance d_{IR}, i.e., (32) is not applicable and the optimal δ has to be found numerically based on (31). Furthermore, the interference components of n_0 and n_{11} are statistically dependent since they originate from the same interference source. However, because of the relatively large distance, d_{ID}, between the interferer and the destination the AWGN is the dominant noise at the destination and the aforementioned dependence can be neglected. In Fig. 7, we show BER vs. P_T/P_I ($P_T = 2P_0 = 2P_1$) for optimal relay placement (ORP) obtained with (31), Gaussian relay placement (GRP) also obtained with (31) but ignoring the non–Gaussian nature of the noise and adopting $\nu = 1$ (valid for Gaussian noise), and equal relay placement (ERP) with $\delta = 0.5$. For OPA the optimal placement was $\delta^* = 0.13$, whereas $\delta = 0.58$ was obtained for GRP. Fig. 7 shows that ORP yields asymptotic performance gains of 1.7 dB and 2.2 dB compared to GRP and ERP, respectively. Furthermore, the simulation results are in excellent agreement with the numerical results indicating that the aforementioned noise dependence which was neglected for the theoretical results but included in the simulations does not have a significant effect.

6 Conclusions

In this paper, we have presented a general analytical framework for the asymptotic analysis of the performance of cooperative diversity systems employing AF relaying in generic noise and interference.

Assuming independent Rayleigh fading for all links, we have derived simple and elegant closed–form expressions for the asymptotic SER and BER in high SNR. Our results are valid for arbitrary linear modulation formats, arbitrary numbers of relays, and all types of noise and interference with finite moments and reveal that while the diversity gain of the system is independent of the type of noise, the combining gain depends on the noise moments of all links. Based on the derived analytical expressions, we have developed power allocation, relay selection, and relay placement strategies that are asymptotically optimal in generic noise and interference. The presented simulation results have confirmed the analysis and have shown that the proposed power allocation, relay selection, and relay placement schemes can lead to significant performance gains in non–Gaussian noise and interference compared to their conventional counterparts which were optimized under the assumption of Gaussian noise.

A Proof of Lemma 2

In this appendix, we prove Lemma 2. While we could reuse some known results from [23] to prove Lemma 1, the proof of Lemma 2 is substantially more difficult and requires more work.

Proof [Lemma 2]: Based on (11) we first rewrite Δ_k, $1 \leq k \leq K$, as

$$\begin{aligned}\Delta_k &= (P_0 A_k^2\, a_{1k}^2\, a_{2k}^2\, d^2 + 2d\sqrt{P_0}\Re\{(A_k\, h_{1k}\, h_{2k})^* \tilde{n}_k\})/\sigma_{\tilde{n}_k}^2 \\ &= P_0 A_k^2\, a_{1k}^2\, a_{2k}^2 d^2/\sigma_{\tilde{n}_k}^2 + 2d\sqrt{P_0}A_k^2 a_{1k} a_{2k}^2 \Re\{\hat{n}_{1k}\}/\sigma_{\tilde{n}_k}^2 + 2d\sqrt{P_0}A_k a_{1k} a_{2k}\Re\{\hat{n}_{2k}\}/\sigma_{\tilde{n}_k}^2\end{aligned} \quad (33)$$

where $\hat{n}_{1k} \triangleq n_{1k}\,\mathrm{e}^{-j\theta_{1k}}$ and $\hat{n}_{2k} \triangleq n_{2k}\,\mathrm{e}^{-j(\theta_{1k}+\theta_{2k})}$. Using the relay gain in (5) and the Taylor series expansion $e^x = \sum_{i=0}^{\infty} x^i/i!$ we obtain

$$\Phi_{\Delta_k}(s|\boldsymbol{n}) = \mathcal{E}_{\boldsymbol{a},\boldsymbol{\theta}}\{e^{-s\Delta_k}\} = \mathcal{E}_{\boldsymbol{a},\boldsymbol{\theta}}\left\{\exp\left(-s\frac{d^2 P_0\, P_k\, a_{1k}^2 a_{2k}^2}{P_0\, a_{1k}^2\, \sigma_{n_{2k}}^2 + P_k\, a_{2k}^2\, \sigma_{n_{1k}}^2}\right) M_k(s)\right\} \quad (34)$$

where we have defined

$$M_k(s) \triangleq \sum_{i=0}^{\infty}\frac{1}{i!}\left(-s2d\sqrt{P_0}A_k^2 a_{1k} a_{2k}^2 \Re\{\hat{n}_1\}/\sigma_{\tilde{n}_k}^2\right)^i \sum_{j=0}^{\infty}\frac{1}{j!}\left(-s2d\sqrt{P_0}A_k a_{1k} a_{2k}\Re\{\hat{n}_2\}/\sigma_{\tilde{n}_k}^2\right)^j. \quad (35)$$

Eq. (35) can be rewritten as the following power series in s:

$$M_k(s) = \sum_{\xi=0}^{\infty} s^{\xi}\,(-2d)^{\xi} \sum_{i+j=\xi}\frac{1}{i!j!}\frac{\gamma_{1k}^{j+i/2}\gamma_{2k}^{i+j/2}}{(\gamma_{1k}+\gamma_{2k})^{j+i}}\frac{\Re\{\hat{n}_{1k}\}^i \Re\{\hat{n}_{2k}\}^j}{\sigma_{n_{1k}}^i \sigma_{n_{2k}}^j}, \quad (36)$$

where we have used (5) and (8). Substituting (36) in (34) yields

$$\Phi_{\Delta_k}(s|\boldsymbol{n}) = \sum_{\xi=0}^{\infty} s^{2\xi}(2d)^{2\xi} \sum_{i+j=\xi} \frac{\beta_i \beta_j}{2i!2j!} \Psi_k^{ij}(d^2 s)|\bar{n}_{1k}|^{2i}|\bar{n}_{2k}|^{2j} \tag{37}$$

with $\beta_i \triangleq \frac{\Gamma(i+1/2)}{\sqrt{\pi}\Gamma(i+1)}$ and

$$\Psi_k^{ij}(s) \triangleq \mathcal{E}_{\gamma_{1k},\gamma_{2k}} \left\{ e^{-s\frac{\gamma_{1k}\gamma_{2k}}{\gamma_{1k}+\gamma_{2k}}} \frac{\gamma_{1k}^{2j+i}\gamma_{2k}^{2i+j}}{(\gamma_{1k}+\gamma_{2k})^{2j+2i}} \right\}. \tag{38}$$

For the derivation of (37) we have used

$$\mathcal{E}_{\theta_{1k}}\{\Re\{\hat{n}_{1k}\}^i\} = \begin{cases} \frac{\Gamma(i/2+1/2)}{\sqrt{\pi}\Gamma(i/2+1)}|n_{1k}|^i, & i \text{ even} \\ 0, & i \text{ odd} \end{cases}, \tag{39}$$

and

$$\mathcal{E}_{\theta_{1k},\theta_{2k}}\{\Re\{\hat{n}_{2k}\}^i\} = \begin{cases} \frac{\Gamma(i/2+1/2)}{\sqrt{\pi}\Gamma(i/2+1)}|n_{2k}|^i, & i \text{ even} \\ 0, & i \text{ odd} \end{cases}. \tag{40}$$

Combining (37) and (42) from Lemma 3 we obtain

$$\begin{aligned} \Phi_{\Delta_k}(s|\boldsymbol{n}) &= \left(\frac{1}{\bar{\gamma}_{1k}} + \frac{1}{\bar{\gamma}_{2k}}\right)\frac{1}{d^2 s} + \sum_{\xi=1}^{\infty} s^{2\xi}(2d)^{2\xi}\left(\frac{\beta_\xi \xi! |\bar{n}_{1k}|^{2\xi}}{2\xi! \bar{\gamma}_{1k}(d^2 s)^{\xi+1}} + \frac{\beta_\xi \xi! |\bar{n}_{2k}|^{2\xi}}{2\xi! \bar{\gamma}_{2k}(d^2 s)^{\xi+1}}\right) \\ &\quad + o\left(\bar{\gamma}_{1k}^{-1}\right) + o\left(\bar{\gamma}_{2k}^{-1}\right). \end{aligned} \tag{41}$$

Finally, using the fact that $2^{2\xi}\beta_\xi(\xi!)^2 = (2\xi)!$ we arrive at (14). □

Lemma 3: For $\bar{\gamma}_{1k}, \bar{\gamma}_{2k} \to \infty$, $\Psi_k^{ij}(s)$ defined in (38) behaves as

$$\Psi_k^{ij}(s) = \begin{cases} \left(\frac{1}{\bar{\gamma}_{1k}} + \frac{1}{\bar{\gamma}_{2k}}\right)\frac{1}{s} + o\left(\bar{\gamma}_{1k}^{-1}\right) + o\left(\bar{\gamma}_{2k}^{-1}\right) & i = j = 0 \\ \frac{j!}{\bar{\gamma}_{2k}\, s^{j+1}} + o\left(\bar{\gamma}_{2k}^{-1}\right) & i = 0, j \neq 0 \\ \frac{i!}{\bar{\gamma}_{1k}\, s^{i+1}} + o\left(\bar{\gamma}_{1k}^{-1}\right) & i \neq 0, j = 0 \\ o\left(\bar{\gamma}_{1k}^{-1}\bar{\gamma}_{2k}^{-1}\right) & i \neq 0, j \neq 0 \end{cases} \tag{42}$$

Proof: The Rayleigh fading assumption implies that γ_{1k} and γ_{2k} are independent and exponentially distributed with mean $1/\bar{\gamma}_{1k}$ and $1/\bar{\gamma}_{2k}$, respectively. Therefore, we can write (38) as

$$\Psi_k^{ij}(s) = \frac{1}{\bar{\gamma}_{1k}\bar{\gamma}_{2k}} \int_0^\infty \int_0^\infty e^{-s\frac{\gamma_{1k}\gamma_{2k}}{\gamma_{1k}+\gamma_{2k}}} \frac{\gamma_{1k}^{2j+i}\gamma_{2k}^{2i+j}}{(\gamma_{1k}+\gamma_{2k})^{2j+2i}} e^{-\frac{\gamma_{1k}}{\bar{\gamma}_{1k}}} e^{-\frac{\gamma_{2k}}{\bar{\gamma}_{2k}}} \mathrm{d}\gamma_{1k}\mathrm{d}\gamma_{2k}. \tag{43}$$

Applying the transformation of variables $\gamma_{1k} = r^2\cos^2\phi$ and $\gamma_{2k} = r^2\sin^2\phi$ in (43) results in

$$\begin{aligned} \Psi_k^{ij}(s) &= \frac{4}{\bar{\gamma}_{1k}\bar{\gamma}_{2k}} \int_0^{\pi/2} \int_0^\infty e^{\left(-s\, r^2 \sin^2\phi \cos^2\phi\right)} r^{2i+2j+3} (\sin^2\phi)^{2i+j+1/2} (\cos^2\phi)^{2j+i+1/2} \\ &\quad \times e^{-r^2\cos^2\phi/\bar{\gamma}_{1k}}\, e^{-r^2\sin^2\phi/\bar{\gamma}_{2k}}\, \mathrm{d}r\, \mathrm{d}\phi. \end{aligned} \tag{44}$$

Using [24, 3.381.4], the above equation reduces to

$$\Psi_k^{ij}(s) \;=\; \frac{2\Gamma(i+j+2)}{\bar{\gamma}_{1k}\bar{\gamma}_{2k}} \int_0^{\pi/2} \Upsilon_k^{ij}(\phi,s)\,\mathrm{d}\phi, \tag{45}$$

where

$$\Upsilon_k^{ij}(\phi,s) \triangleq \frac{(\sin^2\phi)^{2i+j+1/2}(\cos^2\phi)^{2j+i+1/2}}{\left(\sin^2\phi\cos^2\phi\, s+\cos^2\phi/\bar{\gamma}_{1k}+\sin^2\phi/\bar{\gamma}_{2k}\right)^{i+j+2}}. \tag{46}$$

Splitting the integration interval in (45) into three intervals $[0,\epsilon]$, $(\epsilon,\pi/2-\epsilon)$, and $[\pi/2-\epsilon,\pi/2]$, yields

$$\Psi_k^{ij}(s) \;=\; \frac{2\Gamma(i+j+2)}{\bar{\gamma}_{1k}\bar{\gamma}_{2k}}(\mathrm{I}_k+\mathrm{II}_k+\mathrm{III}_k), \tag{47}$$

where $\mathrm{I}_k \triangleq \int_0^{\epsilon}\Upsilon_k^{ij}(\phi,s)\,\mathrm{d}\phi$, $\mathrm{II}_k \triangleq \int_{\epsilon}^{\pi/2-\epsilon}\Upsilon_k^{ij}(\phi,s)\,\mathrm{d}\phi$, $\mathrm{III}_k \triangleq \int_{\pi/2-\epsilon}^{\pi/2}\Upsilon_k^{ij}(\phi,s)\,\mathrm{d}\phi$, and $\epsilon\to 0$ is an arbitrary small positive real number. In the following, we investigate the asymptotic behavior of I_k, II_k, and III_k, respectively, for $\bar{\gamma}_{1k},\bar{\gamma}_{2k}\to\infty$.

Since for $\epsilon\to 0$, $\sin\phi\to\phi$, and $\cos\phi\to 1$ are valid, I_k can be expressed as

$$\mathrm{I}_k = \int_0^{\epsilon} \frac{\phi^{2(2i+j+1/2)}\,\bar{\gamma}_{1k}^{j+i+2}}{\left((s+1/\bar{\gamma}_{2k})\bar{\gamma}_{1k}\phi^2+1\right)^{i+j+2}}\,\mathrm{d}\phi. \tag{48}$$

With the help of [24, 3.194.1] the above equation can be written as

$$\mathrm{I}_k = \frac{\bar{\gamma}_{1k}^{i+j+2}\epsilon^{2(2i+j+1)}}{2(2i+j+1)}\,{}_2\mathcal{F}_1\left(2i+j+1,i+j+2;2i+j+2;-\bar{\gamma}_{1k}(s+1/\bar{\gamma}_{2k})\epsilon^2\right). \tag{49}$$

The asymptotic properties of the Gaussian hypergeometric function ${}_2\mathcal{F}_1(\cdot,\cdot;\cdot;z)$ for $z\to\infty$ [30] can be used to show that for a given ϵ

$$\mathrm{I}_k = \frac{1}{2(2i+j+1)s^{i+j+2}}\left[\frac{\Gamma(1-i)\Gamma(2i+j+2)}{\Gamma(i+j+2)}(\bar{\gamma}_{1k}s)^{-(i-1)}+\frac{2i+j+1}{i-1}\epsilon^{(i-1)}\right]+o\left(\bar{\gamma}_{1k}^{(1-i)^+}\right). \tag{50}$$

where $(x)^+\triangleq\max\{x,0\}$. For III_k similar steps as for I_k can be followed to obtain

$$\mathrm{III}_k = \frac{\bar{\gamma}_{2k}^{i+j+2}\epsilon^{2(2j+i+1)}}{2(2j+i+1)}\,{}_2\mathcal{F}_1\left(2j+i+1,i+j+2;2j+i+2;-\bar{\gamma}_{2k}(s+1/\bar{\gamma}_{1k})\epsilon^2\right), \tag{51}$$

and

$$\mathrm{III}_k = \frac{1}{2(2j+i+1)s^{i+j+2}}\left[\frac{\Gamma(1-j)\Gamma(2j+i+2)}{\Gamma(i+j+2)}(\bar{\gamma}_{2k}s)^{-(j-1)}+\frac{2j+i+1}{j-1}\epsilon^{(j-1)}\right]+o\left(\bar{\gamma}_{2k}^{(1-j)^+}\right). \tag{52}$$

Finally, we employ the *dominated convergence theorem* [31] to show that

$$\mathrm{II}_k = \int_{\epsilon}^{\pi/2-\epsilon} \frac{(\sin^2\phi)^{2i+j+1/2}(\cos^2\phi)^{2j+i+1/2}}{\left(\sin^2\phi\cos^2\phi\, s\right)^{i+j+2}}\,\mathrm{d}\phi = \mu s^{-(i+j+2)}+o\left(1\right), \tag{53}$$

where

$$\mu \triangleq \int_{\epsilon}^{\pi/2-\epsilon} (\sin^2\phi)^{i+j-3/2}(\cos^2\phi)^{j+i-3/2}\mathrm{d}\phi, \tag{54}$$

is a real constant. By combining (50), (52), (53), and (47), and letting first $\bar{\gamma}_{1k}$, $\bar{\gamma}_{2k} \to \infty$ and subsequently $\epsilon \to 0$, we obtain the result in (42). $\square$

References

[1] J. Boyer, D.D. Falconer, and H. Yanikomeroglu. Multihop Diversity in Wireless Relaying Channels. *IEEE Trans. Commun.*, 52:1820–1830, October 2004.

[2] M. Hasna and M.S. Alouini. End-to-End Performance of Transmission Systems with Relays Over Rayleigh–Fading Channels. *IEEE Trans. Wireless Commun.*, 2:1126–1131, November 2003.

[3] W. Limpakom, Y.-D. Yao, and H. Man. Outage Probability Analysis of Wireless Relay and Cooperative Networks in Rician Fading Channels with Different K-Factors. In *Proceedings of IEEE Veh. Technol. Conf.*, pages 1–5, April 2009.

[4] T. Cover and A. El Gamal. Capacity Theorems for the Relay Channel. *IEEE Trans. Inform. Theory*, IT-25:572–584, September 1979.

[5] G. Farhadi and N. Beaulieu. On the Ergodic Capacity of Wireless Relaying Systems over Rayleigh Fading Channels. *IEEE Trans. Wireless Commun.*, 7:4462–4467, November 2008.

[6] J. Laneman, D. Tse, and G. Wornell. Cooperative Diversity in Wireless Networks: Efficient Protocols and Outage Behavior. *IEEE Trans. Inform. Theory*, 50:3062–3080, December 2004.

[7] P. Anghel and M. Kaveh. Exact Symbol Error Probability of a Cooperative Network in a Rayleigh–Fading Environment. *IEEE Trans. Wireless Commun.*, 3:1536–1276, September 2004.

[8] A. Ribeiro, X. Cai, and G. Giannakis. Symbol Error Probabilities for General Cooperative Links. *IEEE Trans. Wireless Commun.*, 4:1264–1273, May 2005.

[9] Y. Zhao, R. Adve, and T.J. Lim. Symbol Error Rate of Selection Amplify–and–Forward Relay Systems. *IEEE Commun. Letters*, 10:757–759, November 2006.

[10] J. Zhang, T. Zhang, J. Huang, and R. Yuan. ABEP of Amplify-and-Forward Cooperation in Nakagami-m Fading Channels with Arbitrary m. *IEEE Trans. Wireless Commun.*, 8:4445–4449, September 2009.

[11] D. Senaratne and C. Tellambura. Unified Exact Performance Analysis of Two Hop Amplify and Forward Relaying in Nakagami Fading. *To appear in IEEE Trans. Vehicular Technology.*, 2010.

[12] Y. Zhao, R. Adve, and T.J. Lim. Improving Amplify–and–Forward Relay Networks: Optimal Power Allocation versus Selection. *IEEE Trans. Wireless Commun.*, 6:3114–3123, August 2007.

[13] D. Xitirnin and A. Haimovich. Power Allocation for Cooperative Relaying in Wireless Networks. *IEEE Commun. Letters*, 9:994–996, November 2005.

[14] B. Maham and A. Hjorungnes. Minimum Power Allocation in SER Constraint Relay Networks. In *Proceedings of IEEE Veh. Technol. Conf.*, pages 2431–2435, May 2008.

[15] T.S. Rappaport. *Wireless Communications*. Prentice Hall, Upper Saddle River, NJ, 2002.

[16] A. Giorgetti and M. Chiani. Influence of Fading on the Gaussian Approximation for BPSK and QPSK with Asynchronous Cochannel Interference. *IEEE Trans. Wireless Commun.*, 4:384–389, March 2005.

[17] R. Prasad, A. Kegel, and A. de Vos. Performance of Microcellular Mobile Radio in a Cochannel Interference, Natural, and Man-Made Noise Environment. *IEEE Trans. Veh. Technol.*, 42:33–40, February 1993.

[18] D. Middleton. Statistical-physical Models of Man–made Radio Noise – Parts I and II. *U.S. Dept. Commerce Office Telecommun.*, April 1974 and 1976.

[19] IEEE P802.15.4a. Wireless Medium Access Control (MAC) and Physical Layer (PHY) Specifications for Low-Rate Wireless Personal Area Networks (LR-WPANs). January 2007.

[20] A. Nasri, A. Nezampour, and R. Schober. Adaptive Lp–Norm Diversity Combining in Non–Gaussian Noise and Interference. *IEEE Trans. Wireless Commun.*, 8:4230–4240, August 2009.

[21] A. Nezampour, A. Nasri, R. Schober, and Y. Ma. Asymptotic BEP and SEP of Quadratic Diversity Combining Receivers in Correlated Ricean Fading, Non–Gaussian Noise, and Interference. *IEEE Trans. Commun.*, 57:1039–1049, April 2009.

[22] E. Biglieri, G. Caire, G. Taricco, and J. Ventura-Traveset. Computing Error Probabilities over Fading Channels: a Unified Approach. *European Trans. Telecommun.*, 9:15–25, Jan./Feb. 1998.

[23] A. Nasri and R. Schober. Performance of BICM–SC and BICM–OFDM Systems with Diversity Reception in Non–Gaussian Noise and Interference. *IEEE Trans. Commun.*, 57:3316–3327, November 2009.

[24] I. Gradshteyn and I. Ryzhik. *Table of Integrals, Series, and Products*. Academic Press, New York, 2000.

[25] J.G. Proakis. *Digital Communications*. McGraw–Hill, New York, forth edition, 2000.

[26] S. Boyd and L. Vandenberghe. *Convex Optimization*. Cambridge, U.K.: Cambridge Univ. Press, 2004.

[27] GGPLAB: A Simple Matlab Toolbox for Geometric Programming. [Online]: http://www.stanford.edu/ boyd/ggplab/.

[28] G. Zeng, P. Voltz, and F. Cassara. Analytical Model of UWB Interference Imposed on Co-Channel Narowband Users. In *Proceedings of the 9th Intern. Conf. on Advanced Commun. Technology (ICACT)*, pages 1926–1930, February 2007.

[29] J. Bellorado, S.S. Ghassemzadeh, L.J. Greenstein, T. Sveinsson, and V. Tarokh. Coexistence of Ultra–wideband Systems with IEEE–802.11 a Wireless LANs. In *Proceedings of the IEEE Global Telecommun. Conf.*, pages 410–414, San Francisco, USA, December 2003.

[30] Wolfram Mathworld. [Online]: http://functions.wolfram.com/ HypergeometricFunctions/Hypergeometric2F1/06/01/05/01/02/.

[31] A. Browder. *Mathematical Analysis: An Introduction*. NewYork: Springer–Verlag, 1996.

Tables and Figures:

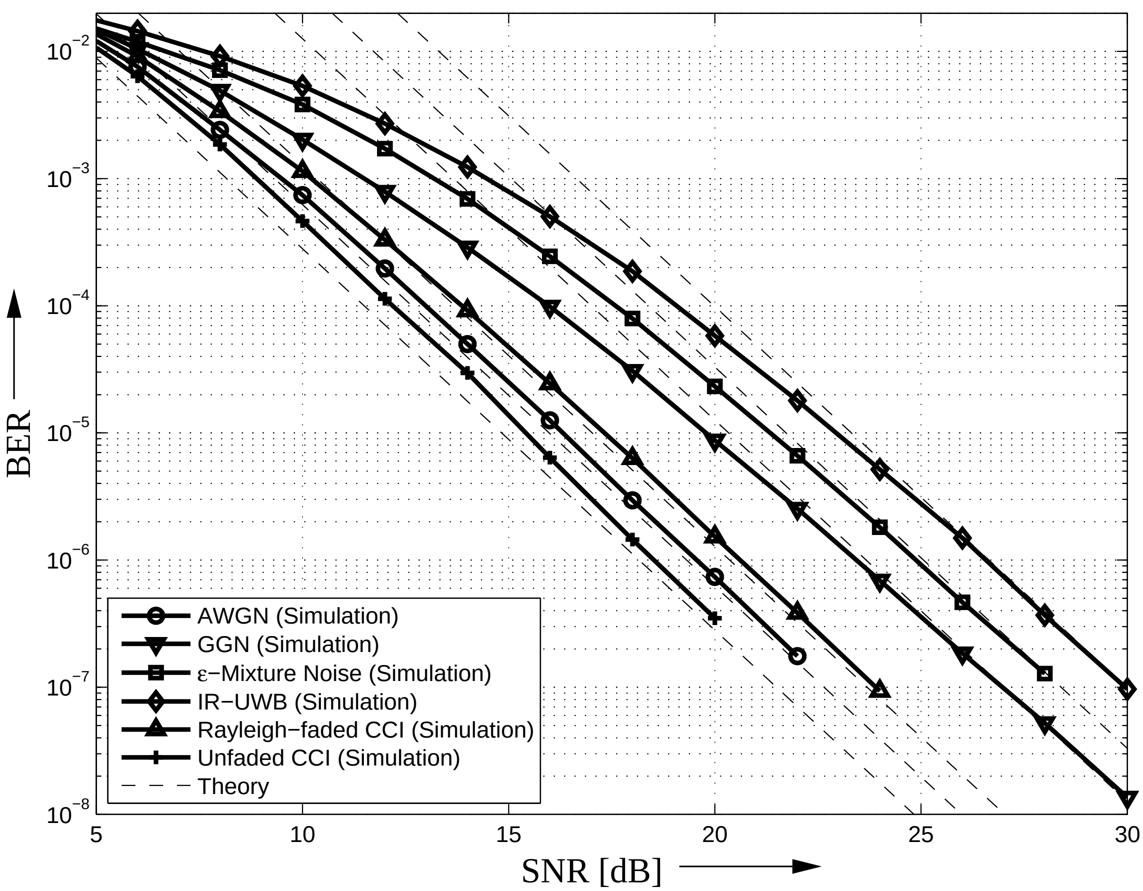

Figure 1: BER vs. SNR γ_t of a cooperative diversity system with $K = 2$ relays and BPSK modulation impaired by various types of noise. Noise parameters (see [20] for the details of the noise models): IR–UWB (bandwidth of victim system $B = 4$ MHz, $N_b = 32$ bursts per IR–UWB symbol and $L_c = 128$ chips per IR–UWB burst), ϵ–mixture noise with parameters $\epsilon = 0.05$ and $\kappa = 50$, GGN with parameter $\beta = 0.5$, and Rayleigh–faded and unfaded 4–PSK CCI with one asynchronous interferer with delay $\tau_1 = 0.25T$ and $\tau_1 = 0$, respectively, where T denotes the symbol duration and raised cosine pulse shaping with roll–off factor 0.3 is assumed (the considered CCI is referred to as CCI–I in [20]). Solid lines with markers: Simulated BER. Dashed lines: Asymptotic BER obtained with (16) and (19).

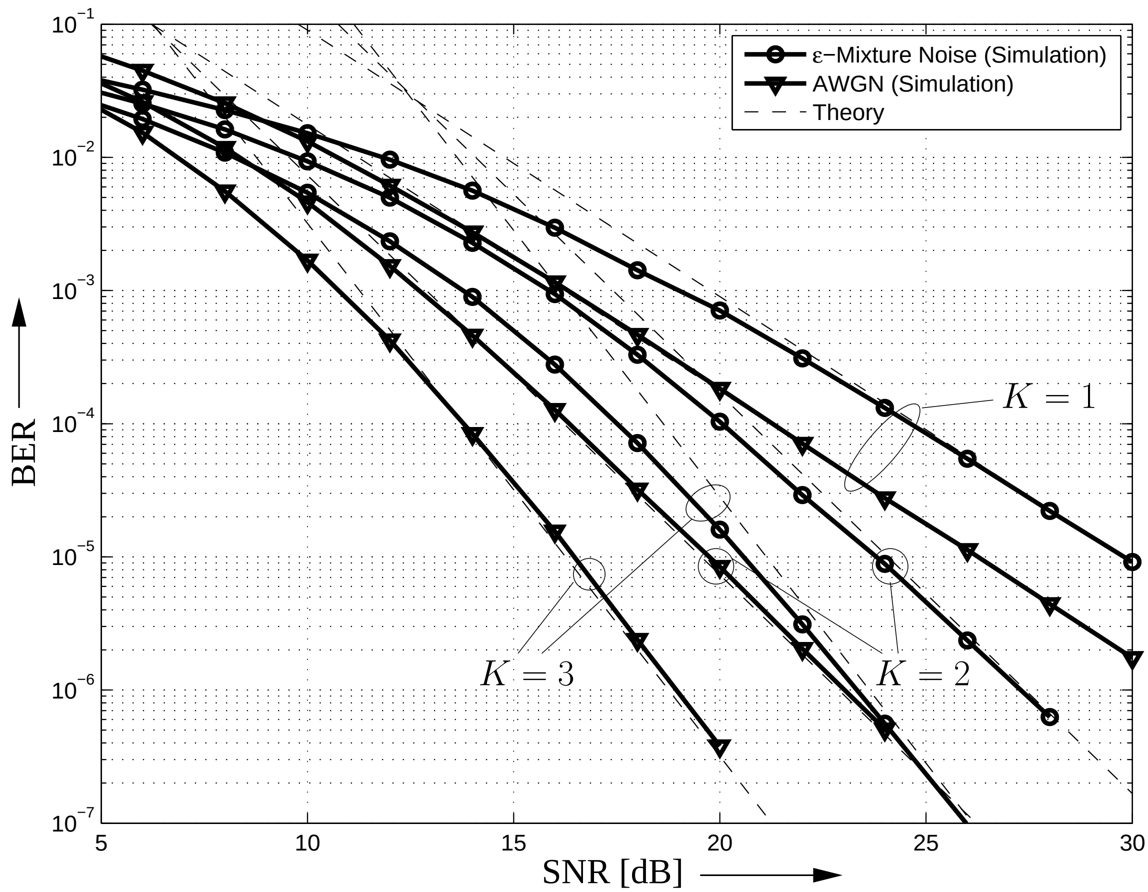

Figure 2: BER vs. SNR γ_t of cooperative diversity systems with different numbers of relays and 16–QAM modulation impaired by ϵ–mixture noise ($\epsilon = 0.1$, $\kappa = 15$) and AWGN, respectively. Solid lines with markers: Simulated BER. Dashed lines: Asymptotic BER obtained with (16) and (19).

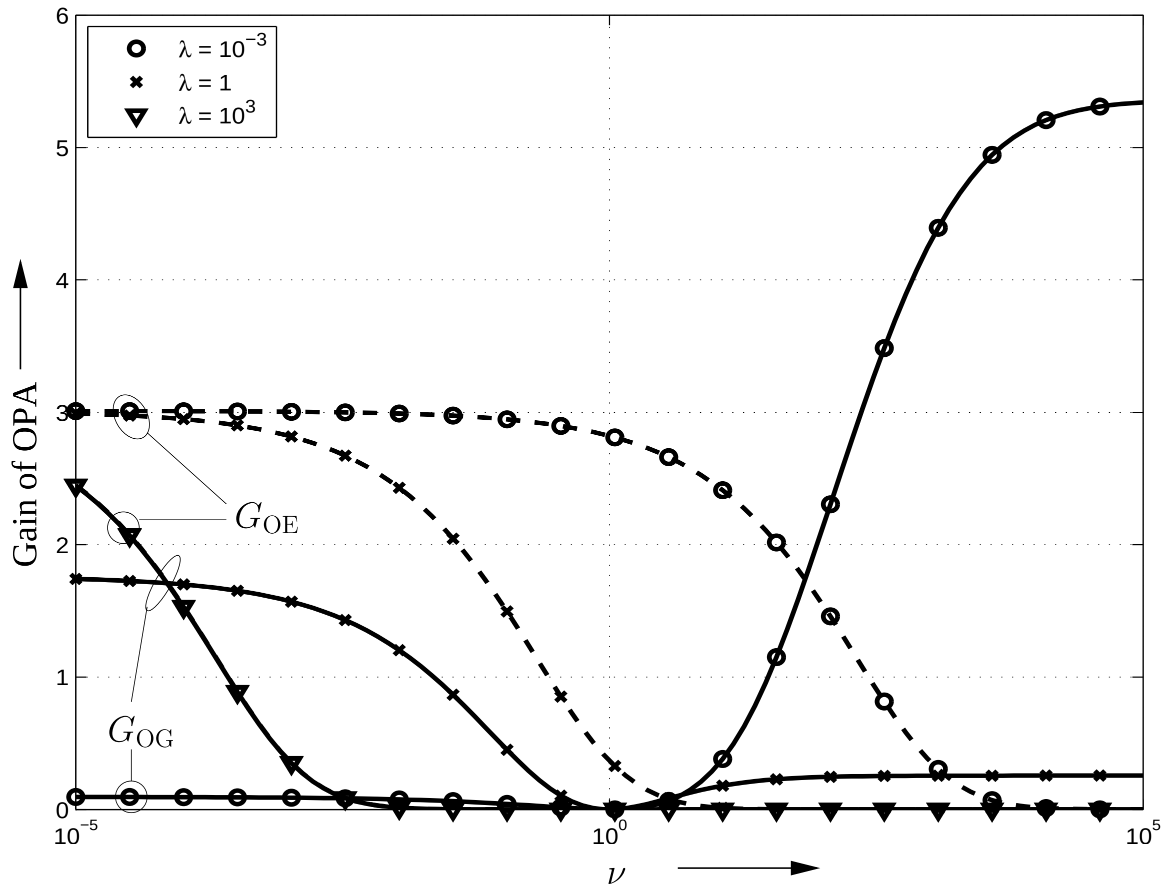

Figure 3: Performance gain of OPA compared to GPA, G_{OG}, and OPA compared to EPA, G_{OE}. The results were obtained from (27) and (28).

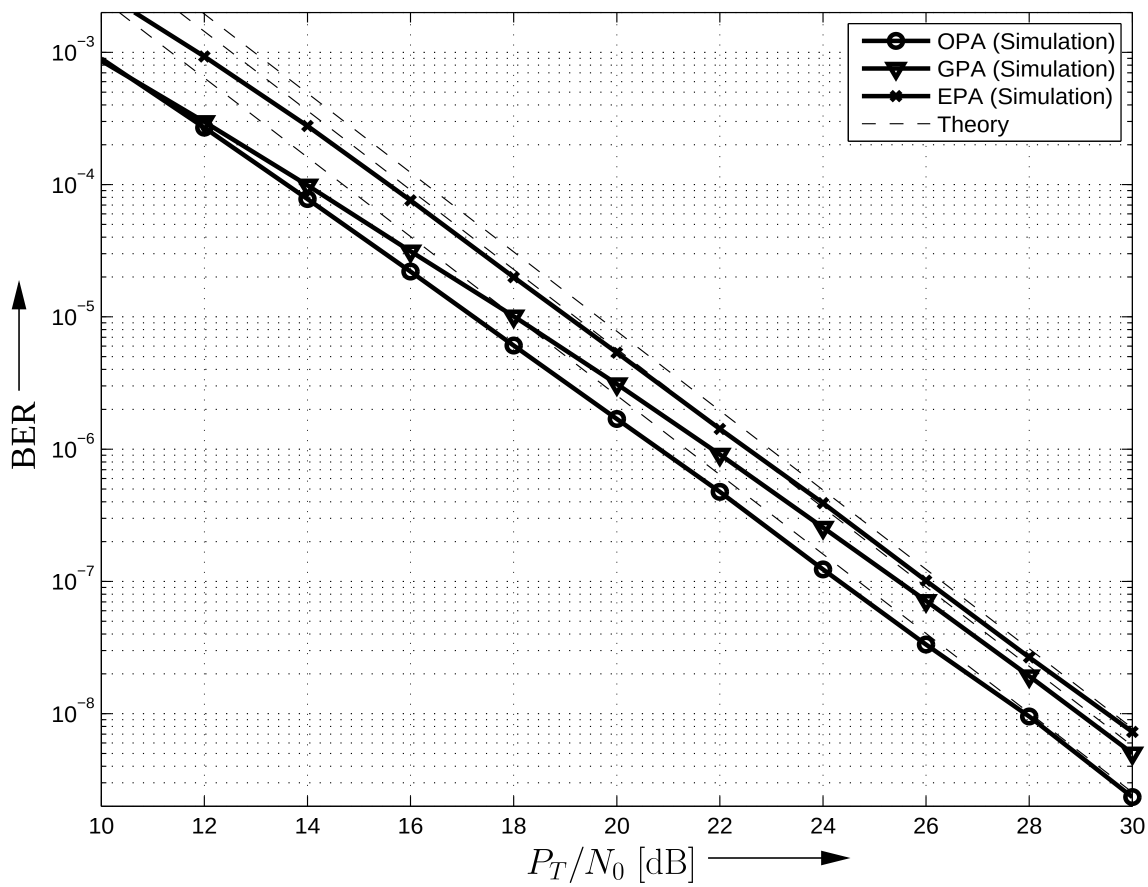

Figure 4: BER vs. P_T/N_0 of a cooperative diversity system with BPSK modulation, $K = 2$ relays, and different power allocation strategies. All links are impaired by AWGN, except the link between the first relay and the destination which is impaired by IR–UWB (bandwidth of victim system $B = 4$ MHz, $N_b = 32$ bursts per IR–UWB symbol, and $L_c = 128$ chips per IR–UWB burst). Solid lines with markers: Simulated BER. Dashed lines: Asymptotic BER obtained with (16) and (19).

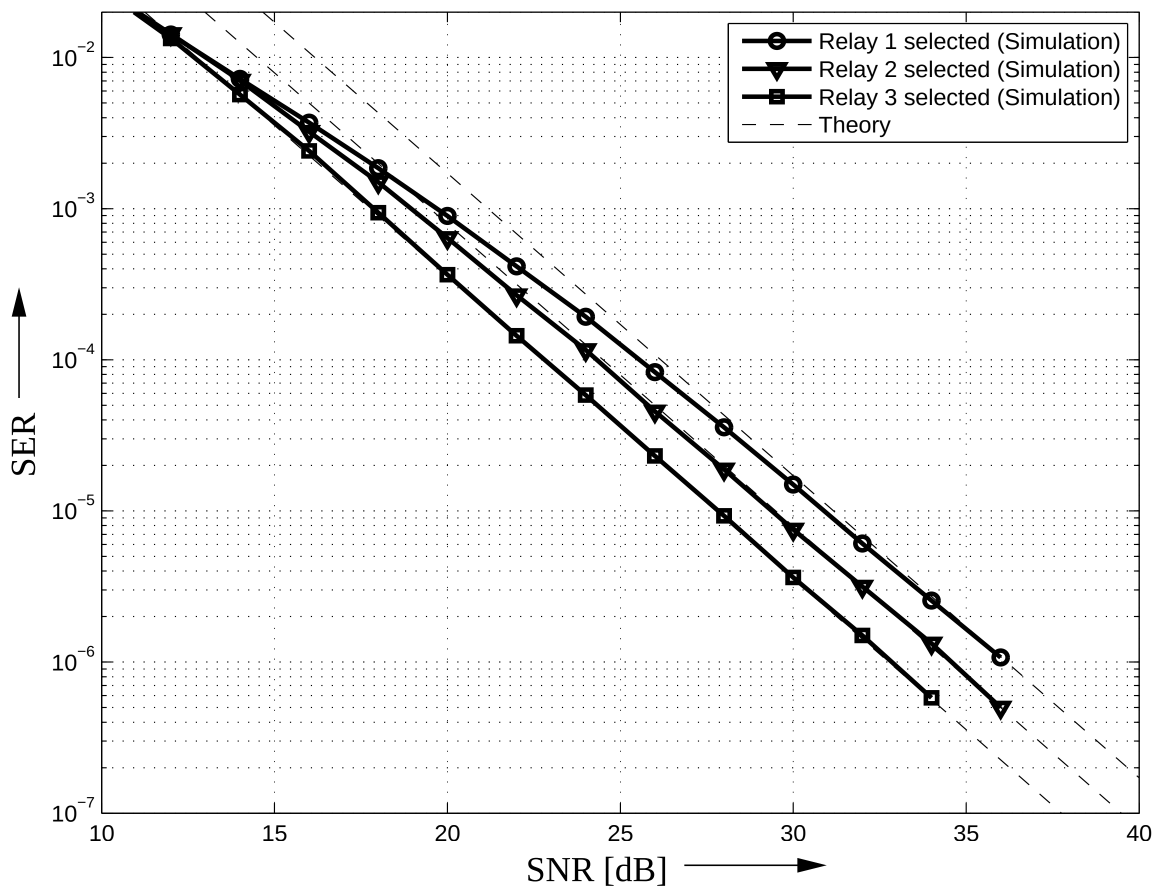

Figure 5: SER vs. SNR γ_t of a cooperative diversity system with 8–PSK modulation and one out of three relays is selected for cooperation. Relays 1, 2, and 3 are impaired by IR–UWB (bandwidth of victim system $B = 4$ MHz, $N_b = 32$ bursts per IR–UWB symbol, and $L_c = 128$ chips per IR–UWB burst), ϵ–mixture noise with parameters $\epsilon = 0.1$ and $\kappa = 50$, and unfaded 4–PSK CCI with one synchronous interferer, respectively. Solid lines with markers: Simulated SER. Dashed lines: Asymptotic SER obtained with (16) and (17).

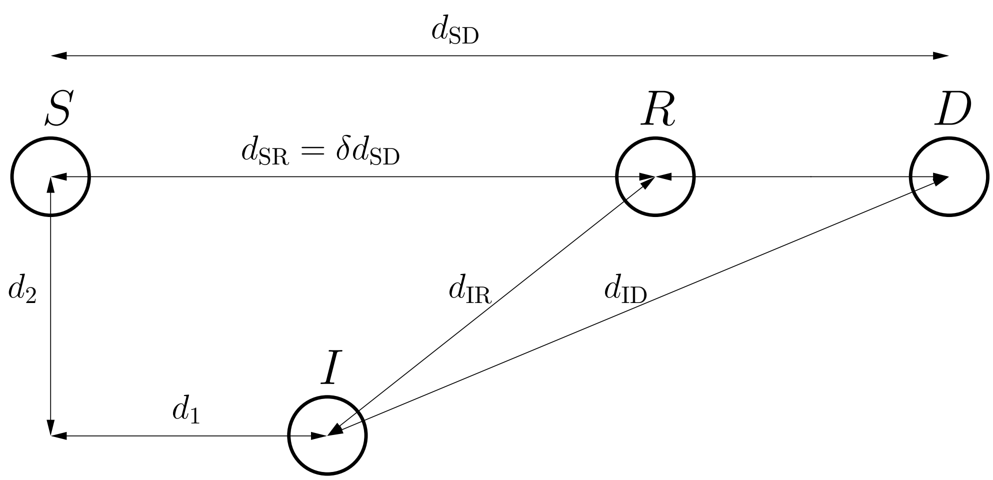

Figure 6: Cooperative diversity system with one source (S), one relay (R), one destination (D), and one impulsive noise emitter (I). For the relay placement results shown in Fig. 7, we assume $d_1 = d_2 = 0.2 d_{\text{SD}}$ for the location of the interferer.

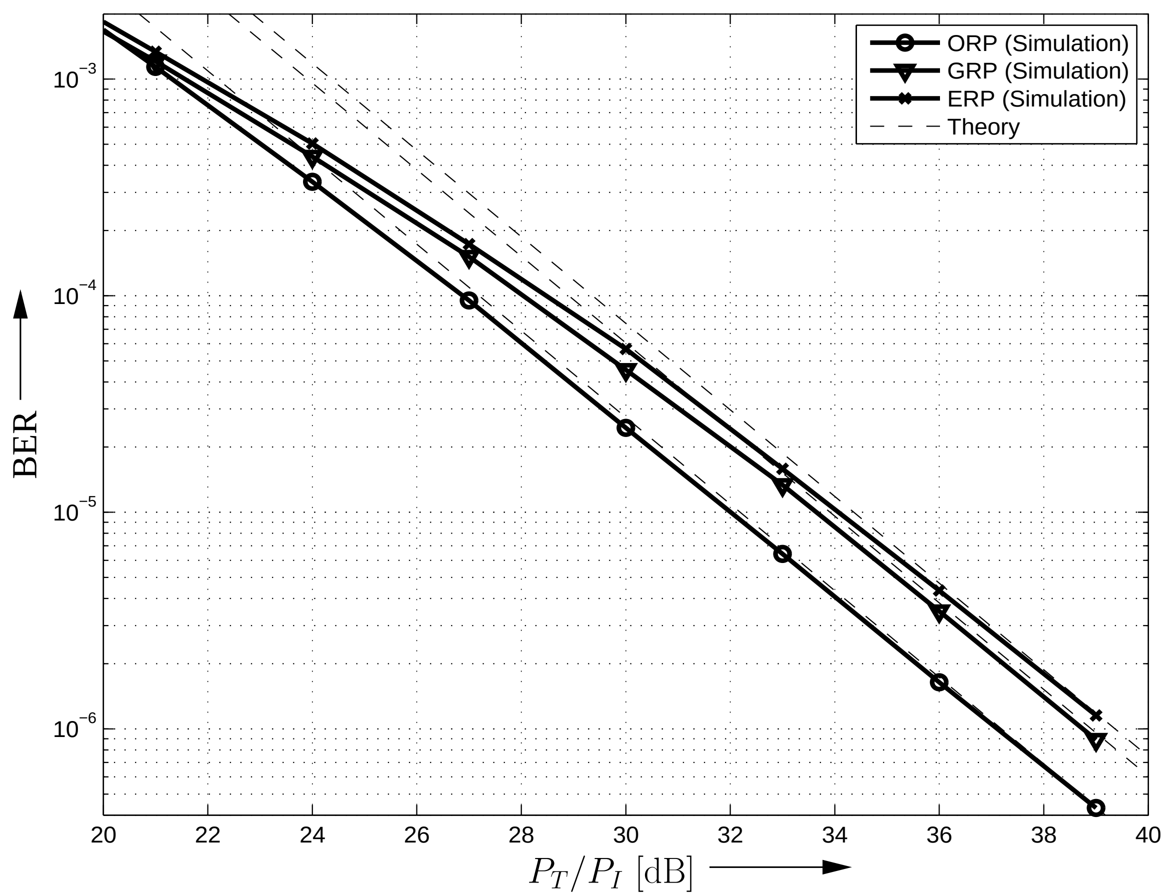

Figure 7: BER vs. P_T/P_I of a cooperative diversity system with BPSK modulation, one relay, and various relay placement strategies. All network nodes are affected by AWGN with $N_0 = -95$ dBm and an impulsive inteferer modeled as ϵ–mixture noise ($\epsilon = 0.01$, $\kappa = 100$) with emitted power $P_I = -58$ dBm. Solid lines with markers: Simulated BER. Dashed lines: Asymptotic BER obtained with (16) and (19).